Journal of Microelectronics and Electronic Packaging (2011) **8**, 1-9

ISSN: 1551-4897

Determination of Electric and Magnetic Properties of Commercial LTCC Soft Ferrite Material

Nelu Blaž,[1,*] Andrea Marić,[1] Goran Radosavljević,[2] Nebojša Mitrović,[3] Ibrahim Atassi,[2] Walter Smetana,[2] and Ljiljana Živanov[1]

***Abstract*—This paper offers an effective, accurate, and simple method for permittivity and permeability determination of an LTCC (low temperature cofired ceramic) ferrite sample. The presented research can be of importance in the fields of ferrite component design and application, as well as for RF and microwave engineering.**

The characterization sample is a stack of LTCC tapes forming a toroid. Commercially available ferrite tape ESL 40012 was used and standard LTCC processing was applied for the sample fabrication. For the first time, the electrical properties of a ferrite toroid sample of ESL 40012 LTCC ferrite tape is presented at various frequencies. The electrical properties of LTCC ferrite materials, permittivity and specific resistivity, are shown in a frequency range from 10 kHz to 1 MHz using the capacitive method. The hysteresis properties of this material are also determined. B-H hysteresis loops were measured applying a maximum excitation of 2 kA/m and frequencies of 50 Hz, 500 Hz, and 1000 Hz.

Permeability is determined in the frequency range from 10 kHz to 1 GHz and a characterization procedure is divided in two segments, for low and high frequencies. Low frequency measurements (from 10 kHz to 1 MHz) are performed using LCZ meter and discrete turns of wire, while a short coaxial sample holder and vector network analyzer were used for the higher frequency range (from 300 kHz to 1 GHz).

In addition, another important factor required for the practical design of devices is presented, the temperature variation of the permeability dispersion parameters.

***Keywords*—LTCC ferrite tape, permeability, permittivity, specific resistivity—**

Introduction

Low temperature cofired ceramic (LTCC) technology has become one of the key technologies for the fabrication of integrated passive devices. Multilayer chip LC filters, multilayer hybrid circuit devices, and chip beads have been introduced in recent years, expanding the family of inductive multilayer devices [1].

As a result of the expansion of devices, the characterization of the electric and magnetic properties of LTCC ferrite material is very important for component design. Knowledge of these parameters can be crucial in circuit design and wave transmission calculations. These materials have many important properties and require different measurement methods for their characterization.

In addition, ferrite materials have extremely nonlinear properties, and a great deal of information can be learned about the magnetic properties of a material by studying its hysteresis loop. There are various methods to determine the hysteresis loop, for example, as shown in Nakmahachalasint et al. [2] and in Tellini et al. [3].

Ferrite's permeability measurements are necessary for engineers to design and choose ferrite properly. The inductance of ferrite core inductors depends not only on the number and geometry of the winding wires, but also on the permeability of the ferrite core. However, at high frequencies, direct measurement of permeability is difficult. The commonly used methods for magnetic material determination are the transmission/reflection method [3-10], the equivalent circuit model method [11, 12], and the resonant method [13]. In Naishadham [11], the frequency dependent RLC equivalent circuit parameters (impedance, resonant frequency, resonant impedance, and quality factor), as well as the effective permeability of the ferrite core, are extracted from the measured values. It is assumed that the capacitance of the equivalent circuit does not vary with frequency. The impedance measurement is accomplished using an impedance analyzer.

Another extraction method, presented in Yu et al. [12], requires the assumption that the inductance of the equivalent circuit does not change significantly with frequency when the frequency is lower than the roll off frequency of core permeability. The equivalent circuit parameters of the inductor are derived by measuring the resonant frequencies of two different inductor circuits where the resonant frequencies are close to each other. Due to the assumptions mentioned above, the upper frequency limitation of this method is the inductor's self-resonant frequency. The measurements must be accomplished using both a network analyzer and an RF LCZ meter. When the relative permeability in the high frequency range extended to 1 GHz or even higher has to be determined, a vector network analyzer (VNA) and an appropriate coaxial sample holder is used acting as a measurement setup [14, 15]. A simple experimental method to determine the initial complex permeability of the toroidal ferrite core using custome designed fixtures is introduced. With the ferrite core installed

Manuscript received May 2011 and accepted July 2011
[1]University of Novi Sad, Faculty of Technical Sciences, Department of Electronics, 2100 Novi Sad, Serbia
[2]Vienna University of Technology, Institute of Sensor and Actuator Systems, A-1040 Vienna, Austria
[3]University of Kragujevac, Technical Faculty Čačak, 3200 Čačak, Serbia
*Corresponding author; email: nelu@uns.ac.rs

doi:10.4071/imaps.286

in a shorted coaxial line, the fixture forms a one turn inductor coil or a shorted transmission line with distributed parameters. The relative permeability of the ferrite can then be extracted from S_{11} of the coaxial test holder with the aid of the vector network analyzer. In addition, the described detailed compensation process is similar to the method presented in Agilent Technologies [16]. A coaxial measurement cell usually consists of a specially shaped composite geometry partially filled with a material sample [17, 18]. Coaxial discontinuity structures are widely used as an element of microwave devices and are commonly used in the permeability and/or permittivity measurement for materials.

Intrinsic complex permeability is the critical parameter for the optimization of design, especially for high frequency applications. In order to achieve better performance of ferrite components, the possibility of their production in LTCC technology is quite attractive from a system design and manufacturing point of view. For the design of ferritic components such as EMI suppressors, it is important to be familiar with the real and imaginary part of the complex permeability. In Wahlers et al. [19] and in Bielawski [20], the frequency variation of the complex permeability modulus of ferrite tape ESL 40010 is demonstrated, but variation of the real and imaginary part of the complex permeability is not shown. Blaž et al. [21] present frequency variation of the real and imaginary part of the complex permeability of ferrite LTCC materials.

Blaž et al. [22] present the hysteresis properties, the estimated effective anisotropy field H_A, the saturation magnetization M_S, and the temperature dependence of permeability dispersion parameters for LTCC ferrite material (ESL 40012) which, to the best of the author's knowledge, did not exist at that time in the available literature. This paper is an improved version of Blaž et al. [22], and for the first time presents the electrical properties of ESL 40012 tape material.

Sample fabrication and material structure are given in the next section. In the following section, measurements of the electric properties for the LTCC ferrite sample are presented. The section after that presents the determination of the hysteresis loop of the fabricated sample. The following section presents the experimental technique for measuring the complex permeability of the toroidal sample in the frequency range from 10 kHz to 1 GHz. After that, the next section presents the determination of the permeability dispersion parameters for ferritic LTCC tape ESL 40012. The last section is Results and Conclusions.

Sample Fabrication and Material Structure

The sample was fabricated using the standard LTCC technology following all conventional steps. Commercial ferrite tape ESL 40012 [23] was used for the sample fabrication and the tapes were structured by means of laser micromachining, laminating, and cofiring the stack of 62 LTCC tape layers. Isostatic lamination of the collated layers was performed at a pressure of 140 bar for 5 min. Firing of the laminated stack was conducted in a high temperature box furnace at a peak temperature of 885°C and a total firing cycle time of 16 h. The finalized sample is presented in Fig. 1. The dimensions of the ferrite sample are: inner diameter 4 mm, outer diameter 6.6 mm, and height 3 mm.

Validation of the structures was performed by optical and electron microscopy. The surface scan shown in Fig. 2 was done by optical microscopy. As can be seen, the glass matrix of the ferrite tape is only partially dissolved at 885°C and some grains have not been fully formed.

Scanning electron micrographs of ESL 40012 LTCC ferrite samples at a magnification of 10000× show grain size, as shown in Fig. 3(a), and the wider view at 1000× is shown in Fig 3(b). As can be seen from Fig. 3(a), the grain size in the sintered ferrite sample varies from 851 nm up to 1.94 μm.

Measurements of Electric Properties for LTCC Ferrite Materials

The electric properties of ferrite materials play an important part in many electronic applications. For example, electrical conductivity promotes eddy currents and prevents high frequency fields from penetrating appreciably below the surface. The permittivity affects the applicability of ferrites to microwave techniques.

It was shown in Heck [24] that the bivalent ferrous ion, when associated in a spinel lattice with the trivalent ion, can substantially lower the resistance. This is to be attributed to the fact that in the spinel lattice, an interchange of electrons can take place very readily between the Fe^{2+} and Fe^{3+} ions.

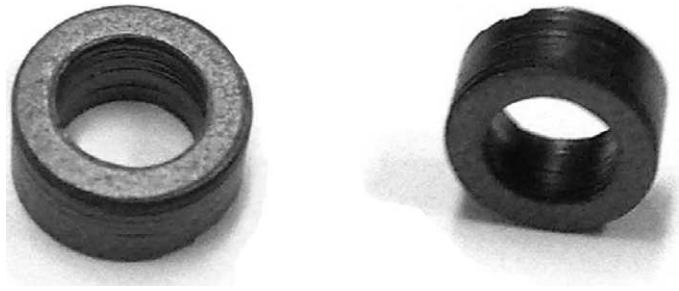

Fig. 1. Toroidal samples formed by 62 layers of ESL 40012 LTCC ferrite tape.

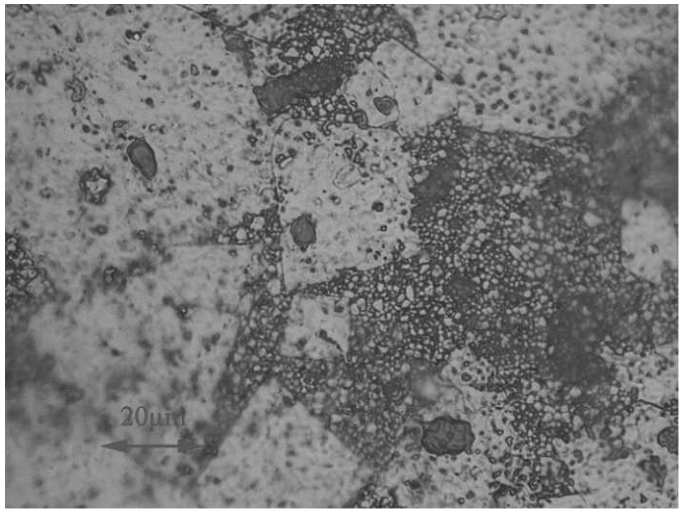

Fig. 2. Surface scan of ESL 40012 LTCC ferrite samples.

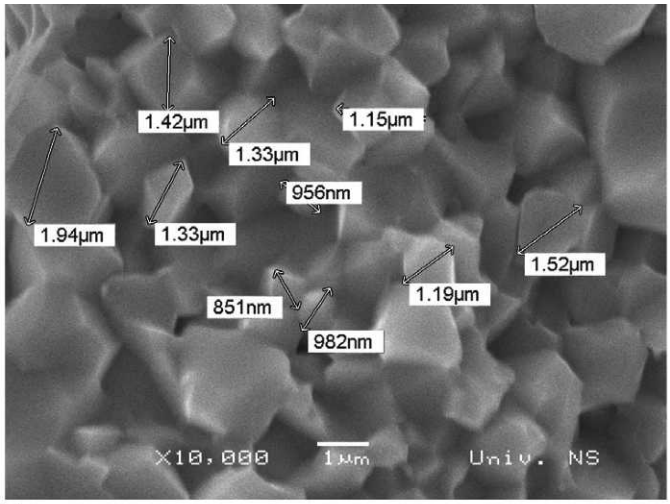

(a)

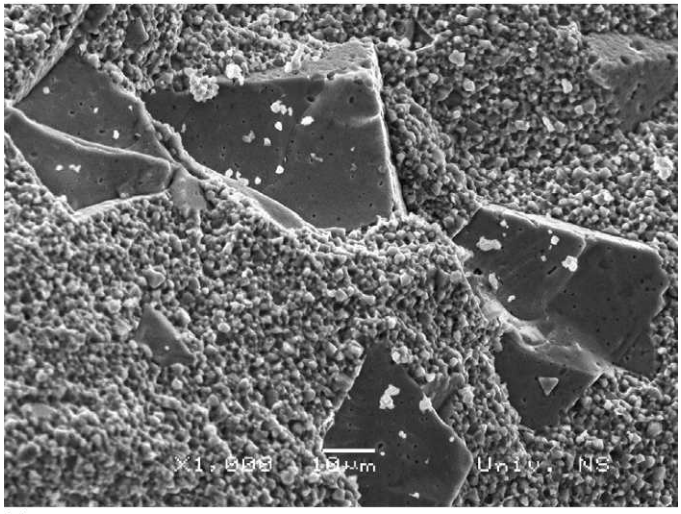

(b)

Fig. 3. SEM micrographs of LTCC ferrite samples: (a) 10,000× magnification showing grain size, and (b) 1000× magnification.

Therefore, ferrites which are to have high electrical resistance, must be free from magnetite.

In previous work, a toroidal sample was used for permeability measurements. Same sample, now, was used for bothpermittivity and specific resistivity measurements. On both sample surfaces, silver paste was applied, as shown in Fig. 4.

The capacitance of the sample was measured (LCZ meter, HP 4277A), and using eq. (1), the permittivity ε_r' was determined

$$\varepsilon_r' = \frac{Cd}{\varepsilon_0(r_2^2 - r_1^2)\pi} \qquad (1)$$

where d is the distance between the plates, C is the capacitance of the sample, ε_0 is the vacuum permittivity, r_2 is the outer radius, and r_1 is the inner radius, as shown in Fig. 5.

The actual calculated values of permittivity for our sample are shown in Fig. 6.

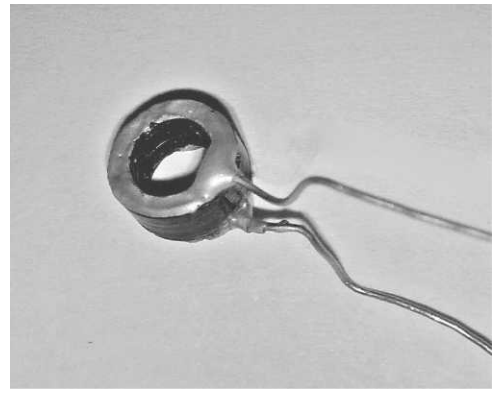

Fig. 4. LTCC ferrite sample prepared for permittivity and specific resistivity determination.

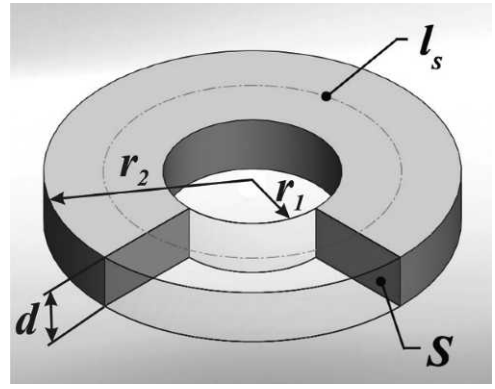

Fig. 5. Cross section of LTCC ferrite sample.

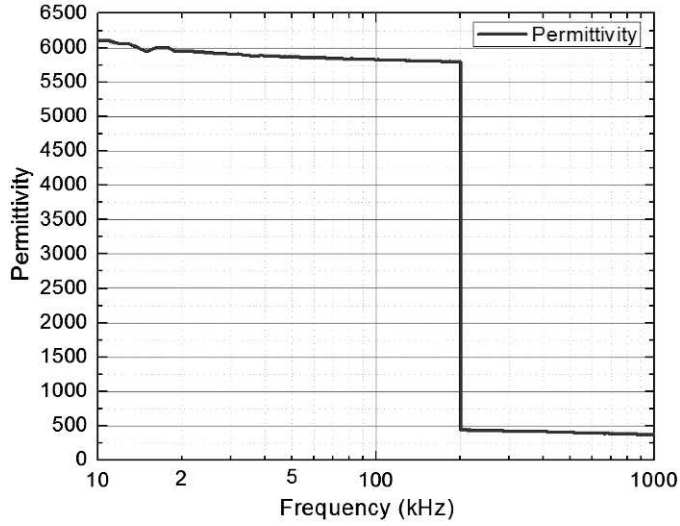

Fig. 6. Characteristic of permittivity versus frequency.

It has been known that ferrites have a high permittivity that depends strongly on frequency. Permittivity slowly decreases from 6200 at 10 kHz to 5800 at 200 kHz. Above 200 kHz, the permittivity falls rapidly from a value of 5800 to 490 and lower.

Using the same LCZ meter, the reactance R of the sample was measured. Employing eq. (2), the specific resistivity ρ of the sample was calculated

$$\rho = \frac{R(r_2^2 - r_1^2)\pi}{d}, \quad (2)$$

where d is the distance between the plates, r_2 is the outer radius, and r_1 is the inner radius, as shown in Fig 5.

The calculated value of the specific electrical resistance of ferrite depends on the measuring frequency as shown in Fig. 7.

It has been found that the permittivity of Ni-Zn ferrite followed much the same course with changing frequency as electrical resistance, that is, it dropped with rising frequency down to a very small value.

The electrical resistance at 200 kHz is only one-eighth of the DC resistance. This resistance drop, which is associated with a similar decrease in permittivity, has led to the proposed ferrite model: ferrite particles are supposed to be individually conducting, relatively speaking, but separated by layers of lower-conductivity material.

Determination of Hysteresis Loop

The complex magnetic permeability and hysteresis characteristic are key parameters that determine the properties of ferrite components.

The magnetic permeability of ferrite materials is not constant, because the relation between the vectors of magnetic induction B and magnetic field H is not linear. The magnetic induction and magnetic moment density of ferrite are not solely a function of the magnetic field strength and do not depend only on the value of field strength at the time of observation, but also on the strength of the field to which the material was previously exposed. This inherently ferromagnetic phenomenon is called hysteresis. Hysteresis can be thought of as a loop formation process. In that meaning, looping is the formation of closed paths in the B-H plane.

In this paper, B-H hysteresis loops were measured by the Brockhaus Tester MPG 100 D (the system meets the requirements of IEC and ASTM and GB standards). The maximum excitation was $H_m = 2$ kA/m using frequencies of 50 Hz, 500 Hz, and 1000 Hz.

The measured hysteresis loops are depicted in Fig. 8 and the relevant numerical values are presented in Table I. As can be seen from Fig. 8, the width of the hysteresis loop expands with an increase in frequency.

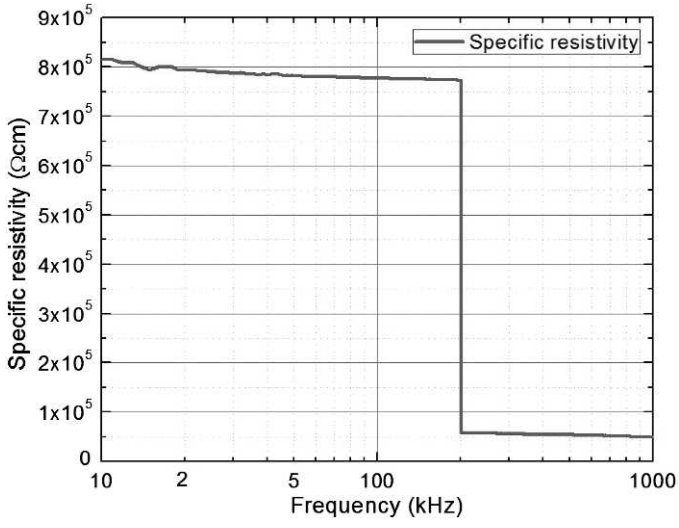

Fig. 7. Specific resistivity versus frequency.

Permeability Measurement

The measurement of complex permeability $(\mu_r = \mu_r' - j\mu_r'')$ will be discussed from two aspects: the frequency range and the applied measurement method.

A. Low Frequency Measurement

Low frequency (10 kHz to 1000 kHz) measurement was performed using an LCZ meter (HP 4277A) and discrete wire turns [15].

The ferrite core with an area of cross section S and an average magnetic path length l_s, Fig. 5, provided with a winding of N turns, can be treated as an impedance $|Z|$ with phase angle Θ and inductance L_s. The complex permeability of the test sample can be calculated from the following equations.

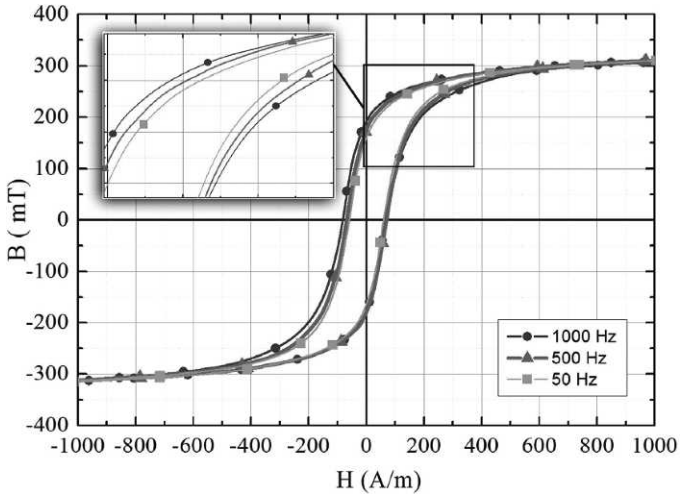

Fig. 8. Hysteresis loops at various frequencies.

Table I
Characteristic Parameters of LTCC Ferrite Samples Obtained from Hysteresis Loop

Frequency (Hz)	H_{max} (A/m)	B_s (mT)	B_r (mT)	H_c (A/m)
50	500	291	157	58
	1000	313	162	59
	2000	329	163	60
500	500	290	163	62
	1000	313	172	66
	2000	327	177	69
1000	500	292	166	63
	1000	313	178	68
	2000	327	184	74

$$\mu_r = \frac{l(L_{s0} - L_s)}{\mu_0 S N^2}, \tag{3}$$

$$\mu_i = \frac{l(|Z|\cos\Theta - |Z_0|\cos\Theta_0)}{\mu_0 \omega S N^2}, \tag{4}$$

where $|Z_0|$, Θ_0, and L_{s0} are parameters measured without the ferrite core, and $|Z|$, Θ, and L_s are parameters measured with the ferrite core. The real and imaginary part of the permeability at low frequency are shown in Fig. 9.

This approach has some disadvantages. First, since the measurement is based on a handmade inductor, measurement results are affected by the winding procedure that was used. If many core samples are measured, repeatability can be a problem due to variation of coil winding.

B. High Frequency Measurement

The most commonly used method for high frequency measurement of complex permeability is the coaxial line method [14, 15].

For higher frequency measurements, we used the E5071B Agilent Technology vector network analyzer with the coaxial sample holder, which consists of a conductive shield surrounding the central conductor, and terminates with short circuit, as can be seen in Fig. 10. This holder has a 50 Ω characteristic impedance and is terminated with a standard APC-7 connector. The medium between the inner and the outer conductor of the cell is air. The height b of the outer conductor is 24.5 mm, which obeys the condition $b < \lambda/4$ for maximum frequency ($f = 1$ GHz) in order to avoid the $\lambda/4$ resonance effect.

The coaxial sample holder (with and without the sample) is connected to the calibrated network analyzer via the 50 Ω coaxial cable. The analyzer supplies an electromagnetic wave propagating in transverse electromagnetic (TEM) mode. The reflection coefficient is measured, permitting the determination of the input impedance of the cell with the sample. The equation for determination of the complex permeability of the holder equipped with the test sample is derived elsewhere [21, 25], and is shown in eq. (5)

$$\tilde{\mu}_r = 1 + \tilde{\chi} = 1 + \frac{\left(\tilde{Z} - \tilde{Z}_{air}\right)}{jh \cdot \mu_0 \cdot f \cdot \ln\left(\frac{d_2}{d_1}\right)}, \tag{5}$$

where d_1 and d_2 denote the inner and outer diameter of the toroid, respectively, h is the height of the toroid, and f is the frequency of the applied electromagnetic field. Therefore, the complex permeability is calculated from the difference between the impedance of the cell loaded with the toroidal sample and without it.

Complex permeability is calculated from the measured S parameters using eq. (5). The real and imaginary parts of ESL 40012 permeability are depicted in Fig. 11.

The maximum value (700) of the the real part of the permeability is found at 2.1 MHz. The imaginary part of the permeability reaches its maximum value (330) at 7 MHz. The intersection of these two characteristics is at 9.3 MHz.

The permeability modulus is presented in Fig. 12 and its peak is 708 at 2.5 MHz. Using eq. (6)

$$tg\delta = \frac{\mu_r''}{\mu_r'}, \tag{6}$$

the loss tangent is calculated and presented in Fig. 13.

The results in Fig. 11 (measured by VNA) have good agreement with characteristics presented Fig. 14 (measured by LCZ), in the frequency range from 300 kHz to 1 MHz.

Based on the permeability model for the demagnetized state proposed by Schlomann [26] for the demagnetized state, the anisotropy field H_A and the saturation magnetization M_S can be calculated with eqs. (7) and (8).

$$H_A = \frac{2\pi \cdot f_{gyromagnetic}}{\mu_0 \cdot \gamma}, \tag{7}$$

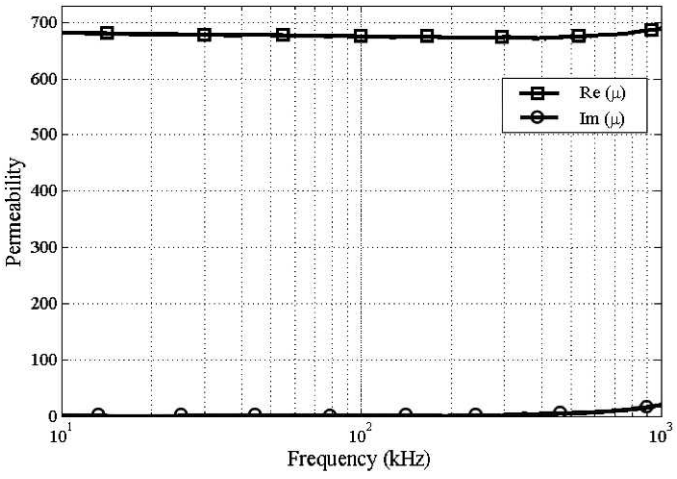

Fig. 9. Real and imaginary part of relative permeability at low frequency.

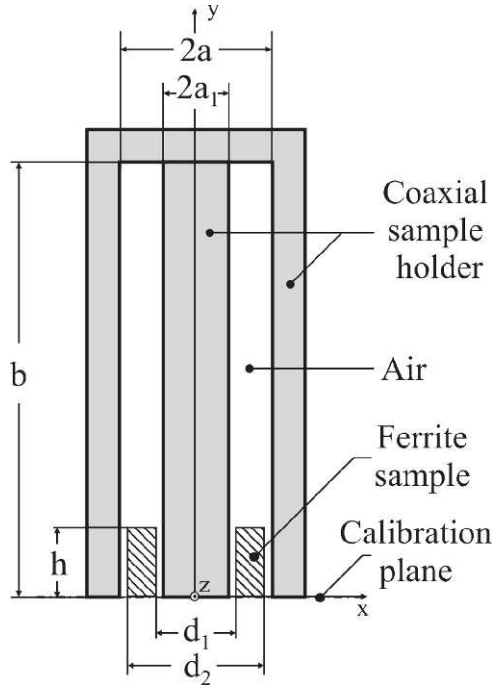

Fig. 10. Cross section of the sample holder with toroidal sample.

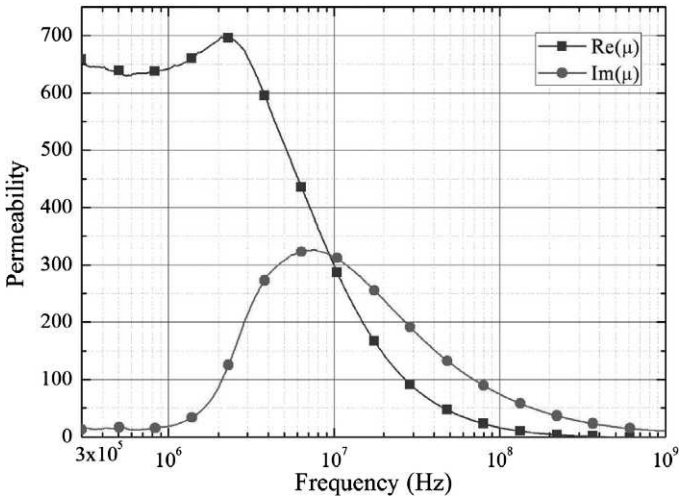

Fig. 11. Real and imaginary part of relative permeability for ESL 40012.

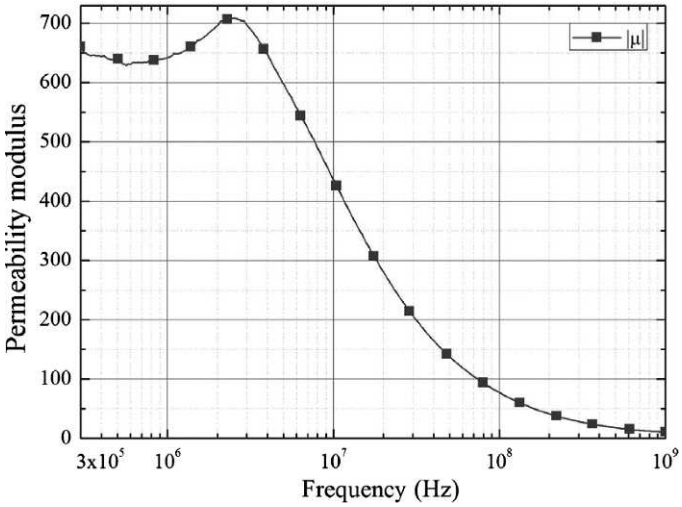

Fig. 12. Permeability modulus of the ferrite tape ESL 40012.

$$M_S = \frac{3}{2}(\mu_r - 1) \cdot H_A. \quad (8)$$

Here $f_{gyromagnetic}$ is the gyromagnetic resonance frequency, γ is the gyromagnetic ratio ($\gamma = 1.8 \times 10^{11}$ Hz/T), and μ_r is the permeability of the demagnetized ferrite at frequencies well below the resonance frequency [27]. The magnetic permeability μ_r was measured at frequencies well below the gyromagnetic resonance frequency $f_{gyromagnetic}$ and its value is 700. The gyromagnetic resonance frequency at which the losses become maximal is 7.8 MHz, as determined from Fig. 11.

Estimates of the effective anisotropy field H_A and the saturation magnetization M_S were derived from the measured values by eqs. (7) and (8) according to Schlomann's model for demagnetized ferrites with ideal domain configurations. The results are summarized in Table II.

The saturation magnetization values lie in the expected values of about 200-300 kA/m. Large-field measurements in a Brockhaus Tester indeed verified the saturation magnetizations within the stated range so that the model assumptions are fulfilled.

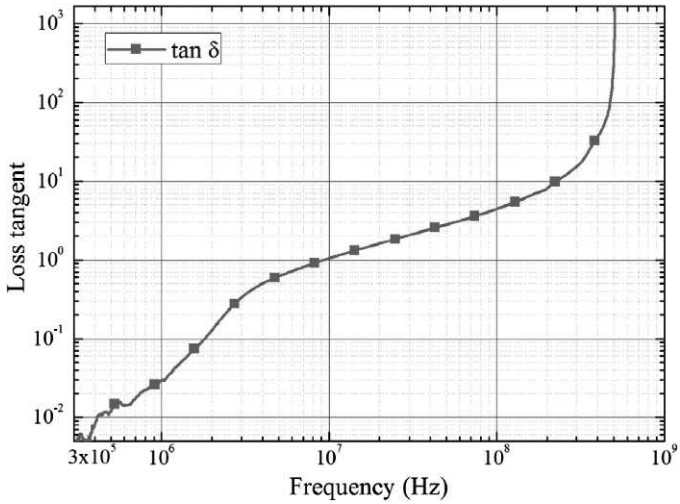

Fig. 13. Loss tangent of the ferrite tape ESL 40012.

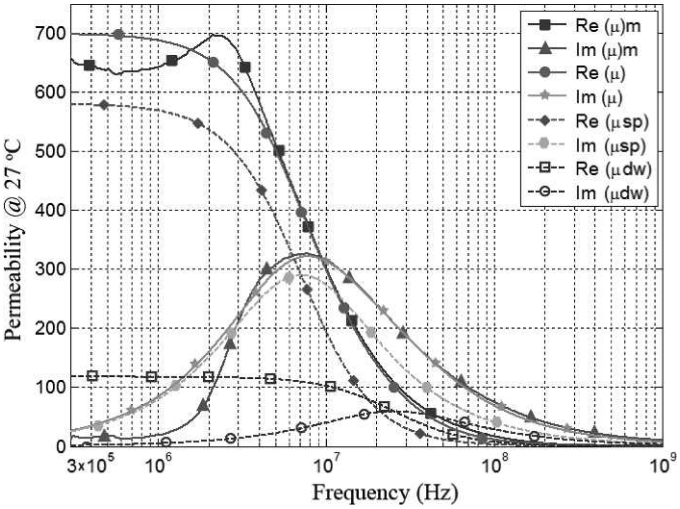

Fig. 14. Comparison between measured and fitted permeability data for ESL 40012 at room temperature.

Table II
Important Parameters of LTCC Ferrite Samples Obtained from Permeability Characteristic

Material	μ_r	$f_{gyromagnetic}$ (MHz)	H_A (kA/m)	M_s (kA/m)	$B_s = \mu_0 * M_s$ (mT)
ESL 40012	700	7.8	216.66	220	276

Temperature Variation of Permeability Dispersion Parameters

Temperature variation of the permeability is another important factor in the practical design in some devices such as

electromagnetic wave absorbers, which require performance stability in outdoor use.

Many ferrite features depend on temperature variation such as permeability. For this reason, additional permeability measurements were performed in the same considered frequency range, but at a variety of temperatures. The variation of the real and imaginary part of the permeability spectra with temperature is presented elsewhere [21, 28, 29].

It is well known that permeability spectra of polycrystalline ferrites can be decomposed into a spin rotational component and a domain wall motion component. The real and imaginary parts of permeability have been separated, and they can be expressed as:

$$\mu' = 1 + \frac{K_{\text{spin}}\left(\omega_{\text{spin}}^{\text{res}}\right)^2}{\left(\omega_{\text{spin}}^{\text{res}}\right)^2 + \omega^2} + \frac{K_{\text{dw}}\left(\omega_{dw}^{res}\right)^2\left(\left(\omega_{\text{dw}}^{\text{res}}\right)^2 - \omega^2\right)}{\left(\left(\omega_{\text{dw}}^{\text{res}}\right)^2 - \omega^2\right)^2 + \beta^2\omega^2}, \quad (9)$$

$$\mu'' = \frac{K_{\text{spin}}\omega_{\text{spin}}^{\text{res}}\omega}{\left(\omega_{\text{spin}}^{\text{res}}\right)^2 + \omega^2} + \frac{K_{\text{dw}}\left(\omega_{\text{dw}}^{\text{res}}\right)^2\beta\omega}{\left(\left(\omega_{\text{dw}}^{\text{res}}\right)^2 - \omega^2\right)^2 + \beta^2\omega^2}, \quad (10)$$

where ω is the operating frequency, K_{spin} is the static spin susceptibility, $\omega_{\text{spin}}^{\text{res}}$ is the spin resonance frequency, K_{dw} is the static susceptibility of domain wall motion, $\omega_{\text{dw}}^{\text{res}}$ is the domain wall resonance frequency, and β is the damping factor of the domain wall motion.

Table III
Permeability Dispersion Parameters of LTCC Ferrite Material for Spin and Domain Wall Resonance at Various Temperatures

ESL 40012	K_{spin}	$\omega_{\text{spin}}^{\text{res}}$	K_{dw}	$\omega_{\text{dw}}^{\text{res}}$	β
@ 27 °C	590	7 MHz	118	63.2 MHz	155.7×10^6
@ 50 °C	591	6.5 MHz	118	60 MHz	150×10^6
@ 70 °C	590.5	5.8 MHz	118	58 MHz	143.4×10^6
@ 100 °C	580	3.9 MHz	115	38 MHz	70.8×10^6
@ 120 °C	490	3.6 MHz	88	35 MHz	70×10^6

Using the developed model, all dispersion parameters can be determined by numerical fitting to specified curves. For faster determination of dispersion parameters, special software was developed.

As can be seen from the measured results and fitted characteristics, there is a good match in the frequency range from 50 MHz to 1 GHz, implying the accuracy of the presented model in this frequency range. The real and imaginary part of measured and fitted characteristics intersect at the same frequency, 9.3 MHz.

For further analysis with the proposed model, the dispersion parameters are determined at various temperatures. Table III shows the fitted values of the dispersion parameters that coincide with the experimental curves given in Blaž et al. [21].

Spin and domain wall resonance frequency with temperature, as shown in Figs. 15(a) and 15(b) decrease with

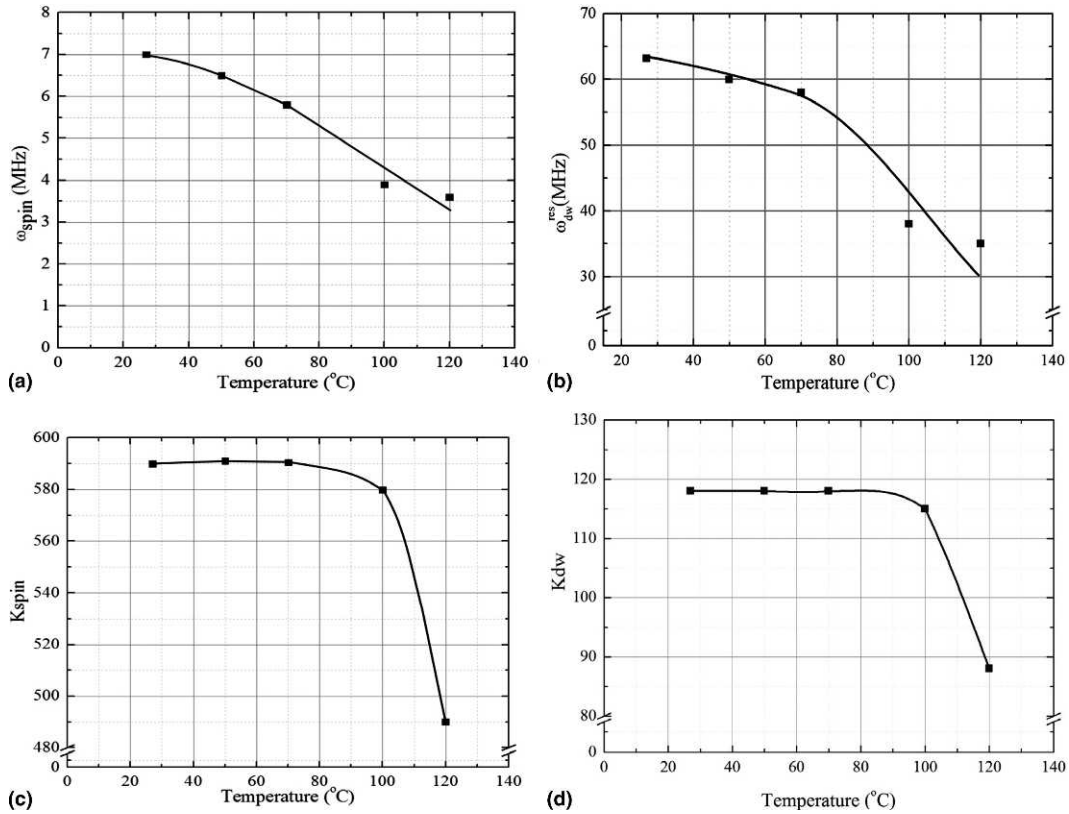

Fig. 15. Temperature dependence of: (a) spin resonance frequency $\omega_{\text{spin}}^{\text{res}}$, (b) domain wall resonance frequency $\omega_{\text{dw}}^{\text{res}}$, (c) spin susceptibility K_{spin} and (d) static susceptibility of the domain wall motion K_{dw}, for the LTCC sample.

increase of temperature. Figs. 15(c) and 15(d) present the temperature dependence of spin susceptibility K_{spin} and static susceptibility of the domain wall motion K_{dw}. As can be seen from the characteristics, the values decrease rapidly beyond a temperature of 100°C. A similar trend for these parameters is shown in Tsutaoka et al. [28]. However, although Ni-Cu-Zn ferrites have successfully been produced for multilayer inductors, there are still unresolved issues that require further investigation, for example, stresses of internal windings, compatibility with Ag, silver mobility in the ferrite, and others [30].

Discussion and Conclusion

In this paper we present both electrical and magnetic properties of commercially available LTCC tape of soft ferrite material. For the first time, the electrical properties of a ferrite toroid sample of ESL 40012 LTCC ferrite tape, at various frequencies, is shown. The toroidal sample was fabricated using conventional LTCC technology of 62 LTCC tape layers. Permittivity and specific resistivity of the toroid sample was determined in the frequency range from 10 kHz to 1MHz. The permeability in the frequency range of 10 kHz to 1 MHz was measured on a wire-wound toroid using an LCZ meter. For frequencies of 300 kHz to 1 GHz, the toroid was measured with a vector network analyzer and a coaxial sample holder. The obtained permeability results show good agreement when they are compared with the manufacturer's data sheet (permeability at 100 kHz is higher than 450). Permeability dispersion parameters are determined by numerical fitting of the obtained experimental results. Also, we presented the temperature dependence of the permeability dispersion parameters for better characterization of the material.

Acknowledgment

This work was done within the scope of two projects, EUREKA project IPCTECH, No. E!4570. and incorporated in project of Ministry of Science and Technological Development, Republic of Serbia, TR 32016.

References

[1] J. Töpfer, J. Mürbe1, A. Angermann, S. Kracunovska, S. Barth, and F. Bechtold, "Soft ferrite materials for multilayer inductors," International Journal of Applied Ceramic Technology, Vol. 3, No. 6, 2006, pp. 455-462,

[2] P. Nakmahachalasint and K.D.T. Ngo, "High-temperature, high-frequency characterization system for power ferrites," IEEE Transactions on Instrumentation and Measurement, Vol. 52, No. 3, 2003, pp. 804-808

[3] B. Tellini, R. Giannetti, and S. Lizón-Martínez "Sensorless measurement technique for characterization of magnetic material under nonperiodic conditions" IEEE Transactions on Instrumentation and Measurement, Vol. 57, No. 7, 2008, pp1465-1469

[4] W.B. Weir, "Automatic measurement of complex dielectric constant and permeability at microwave frequencies," Proceedings of the IEEE, Vol. 62, 1974, pp. 33-36

[5] Hewlett-Packard, "HP Product Note 8510-3, Measuring dielectric constant with the HP 8510 Network Analyzer: The measurement of both permittivity and permeability of solid materials." HP Literature No. 5954-1535, 1985.

[6] V. Chukhov, "Method of magnetic permeability measurement," 14th International Crimean Conference on Microwave and Telecommunication Technology, CriMico,2004, pp. 680-681.

[7] H.B. Bussey, "Measurement of RF properties of materials: A survey," Proceedings of the IEEE, Vol. 55, No. 6, 1967, pp. 1046-1053

[8] W. Barry, "A broad-band, automated, stripline techniques for the simultaneous measurement of complex permittivity an permeability," IEEE Transactions on MTT, Vol. 34, No.1, 1986, pp. 80-84

[9] J.B. Jarvis, M.D. Janezic, B.F. Riddle, R.T. Johnk, R. Kabos, C.L. Holloway, R.G. Geyer, and C.A. Grosvenor, "Measuring the permittivity and permeability of lossy materials: solids, liquids, metals, building materials, and negative-index materials," NIST Technical Note 1536, Boulder, CO, 2005.

[10] Y.Q. Wu, , Z.X. Tang, Y.H. Xu, and B. Zhang, "Measuring complex permeability of ferromagnetic thin films using microstrip transmission method," Journal of Electromagnetic Waves and Applications, Vol. 23, No. 10, 2009, pp. 1303-1311

[11] K. Naishadham, "A rigorous experimental characterization of ferrite inductors for RF noise suppression," 1999 IEEE Radio and Wireless Conference, RAWCON 99, 1999, pp. 271-274.

[12] Q. Yu, T.W. Holmes and K. Naishadham, "RF equivalent circuit modeling of ferrite-core inductors and characterization of core materials," IEEE Transactions Electromagnetic Compatibility, Vol. 44, No. 1, pp. 258-262, Feb. 2002.

[13] C. F. Foo and D. M. Zhang, "A resonant method to construct core loss of magnetic materials using impedance analyzer," in PESC 98, the 29th Annual IEEE Power Electronics Specialists Conference, Vol. 2, 1998, pp. 1997-2002.

[14] J. Shenhui and J. Quanxing, "An alternative method to determine the initial permeability of ferrite core using network analyzer," IEEE Transactions on Electromagnetic Compatibility, Vol. 47, No. 3, 2005, pp. 651-657

[15] R. Dosoudil, E. Ušak, and V. Olah, "Computer controlled system for complex permeability measurement in the frequency range of 5Hz-1GHz," Journal of Electrical Engineering, Vol. 57, No. 8/S, 2006, pp. 105-109.

[16] Agilent Technologies, "Agilent 16454A Magnetic Material Test Fixture Operation and Service Manual," Agilent Technologies, Inc., Palo Alto, CA, 5th ed., Agilent Tech. Rep., No. 16454-90020, July 2001.

[17] J. Huang, K. Wu, P. Morin, C. Akgel, "Characterization of highly dispersive materials using composite coaxial cells: Electromagnetic analysis and wideband measurement," IEEE Transactions on Microwave Theory and Techniques, Vol. 44, No. 5, pp. 770-777, 1996.

[18] D.M. Zhang and C.F. Foo "Theoretical analysis of the electrical and magnetic field distribution in a toroidal core with circular cross section," IEEE Transactions on Magnetics, Part 2, Vol. 33, No. 3, pp. 1924-1931, 1999.

[19] R.L. Wahlers, C.Y.D. Huang, M.R. Heinz, A.H. Feingold, J. Bielawski, and G. Slama, "Low profile LTCC transformers." Available at www.electroscience.com/publications/IMAPS2002(1).pdf.

[20] J. Bielawski, G.A. Slama, A.H. Feingold, C.Y.D. Huang, M.R. Heinz, R.L. Wahlers, "Low Profile Transformers Using Low Temperature Co-Fired Magnetic Tape", Proceedings of the IMAPS 2002 Telecom Hardware Solutions Conference.

[21] N. Blaž, A. Marić, G. Radosavljević, L. Živanov, G. Stojanović, I. Atassi, and W. Smetana, "Modeling and characterization of frequency and temperature variation of complex permeability of ferrite LTCC material," *Progress in Electromagnetics Research B*, Vol. 23, 131-146, 2010.

[22] N. Blaž, A. Marić, G. Radosavljević, N. Mitrović, I. Atassi, W. Smetana, and Lj. Živanov, "Wide frequency characterization of magnetic properties of commercial LTCC ferrite material," IMAPS/ACerS 7th CICMT International Conference and Exhibition, 2011, pp. 224-231.

[23] ESL ElectroScience. Available at http://www.electroscience.com

[24] C. Heck, "Magnetic Materials and Their Applications," New York: Crane, Russak & Co., Inc., 1974.

[25] V. Radonić, N. Blaž, and L. Živanov, "Measurement of complex permeability using short coaxial line reflection method," Acta Physica Polonica, Vol. 117, No. 5, 2010, pp. 820-824

[26] E. Schlomann, Microwave behavior of partially magnetized ferrites. Journal of Applied Physics Vol. 41, No. 1, 1970, pp. 204-214.
[27] M. Matters-Kammerer, U. Mackens, K. Reimann, R. Pietig, D. Hennings, B. Schreinemacher, R. Mauczok, S. Gruhlke, and C. Martiny, Material properties and RF applications of high k and ferrite LTCC ceramics, Microelectronics Reliability, Vol. 46, No. 1, pp. 134-143, 2006.
[28] T. Tsutaoka, M. Ueshima, and T. Tokunaga, "Frequency dispersion and temperature variation of complex permeability of Ni-Zn ferrite composite materials," Journal of Applied Physics, Vol. 78, No. 6, pp. 3983-3991, 1995.
[29] T. Tsutaoka, "Frequency dispersion of complex permeability in Mn-Zn and Ni-Zn spinel ferrites and their composite materials," Journal of Applied Physics, Vol. 93, No. 5, pp. 2789-2796, 2003.
[30] J. Murbe and J. Topfer, "Mg-CuZn ferrites for multilayer inductors," International Journal of Applied Ceramics Technology, Vol. 4, No. 5, pp. 415-422, 2007.